RSC Advances

ROYAL SOCIETY OF CHEMISTRY

www.rsc.org/advances

Heterogeneous catalysis of transesterification *Jatropha curcas* oil over calcium cerium bimetallic oxide catalyst

Siow Hwa Teo,[a, b] Umer Rashid,[a, b] Yun Hin Taufiq-Yap[a, b, c]

[a] Catalysis Science and Technology Research Centre, Faculty of Science, Universiti Putra Malaysia, 43400, UPM Serdang, Selangor, Malaysia.

[b] Department of Chemistry, Faculty of Science, Universiti Putra Malaysia, 43400, UPM Serdang, Selangor, Malaysia.

[c] Institute of Advanced Technology, Universiti Putra Malaysia, 43400 UPM Serdang, Selangor, Malaysia.

Yun Hin Taufiq-Yap (**Corresponding author**)
Catalysis Science and Technology Research Centre,
Faculty of Science, Universiti Putra Malaysia, 43400,
UPM Serdang, Selangor, Malaysia.
Tel: +603-89466809, Fax: +603-89466758,
Email: taufiq@upm.edu.my

A series of heterogeneous basic catalysts (mixed oxides of Ca and Ce) with different molar ratios were synthesized via conventional co-precipitation process using super alkaline carbonate salt. Moreover, investigation was done batchwise for transesterification of crude *Jatropha curcus* oil (JCO) with methanol at 65 °C and 1 atm pressure. The bimetallic oxides posses' high thermal stability, since X-ray diffraction (XRD) proved that the crystalline phases present in mixed oxide catalysts preserved well as pure oxide even up to 900 °C. The co-precipitation synthesis method provided better interaction between vacancies created by the substitution of calcium (Ca) and cerium (Ce) at pH 11. Besides, the combination of Ca and Ce reduced the temperature maxima and increased basicity of catalysts which exhibited better catalytic activity compared with bulk catalysts (CaO and CeO_2). Influences of Ca/Ce atomic ratio in the mixed oxide catalyst, methanol/oil molar ratio, catalyst amount and reaction time on the fatty acid methyl ester (FAME) content were studied. The suitable molar ratio of Ca-to-Ce was 1, and the optimum condition of 4 wt. % catalyst dosages and 15 % methanol/oil molar ratio, the fatty acid methyl ester (FAME) content of 95% was achieved over CaO-CeO_2 catalyst at 65 °C. Additionally, CaO-CeO_2 catalyst shows substantial chemical stability and could be reused for at least 4 times without major loss in its catalytic activity.

Keywords Ca/Ce molar ratio; high stability; *Jatropha curcas* oil; mixed metal oxides; transesterification.

Introduction

The growing energy demands of mankind, due to the depletion of world's petroleum reserves and environmental issues. Therefore, there is a great challenge for researchers in finding alternative sources for petroleum based fuels. At the present, the conversion of biomass into renewable transportation fuels is receiving more and more attention.[1,2] Production of hydrogen from cellulose,[3] fermentation of sugar to bioethanol[4] and transesterified of vegetable oil or fats into biodiesel[1,2,5] are up to date.

Biodiesel is a clean renewable fuel and it can be used in any compression ignition engine without modification.[6] Recently, more than 95 % of biodiesel production feedstocks come from edible vegetable oils and the properties of biodiesel produced from these candidates are much suitable to be used as diesel fuel replacement.[1,7]

The potential of non-edible oils has not been considered as alternative feedstock for biodiesel production. Many researchers are interested in non-edible oil sources (non-food vegetable oils, animal fats and waste oils) to be renewable and sustainable solution.[8,9] *Jatropha curcas* oil (JCO) is considered to be a promising feedstock which is low cost and non-food based feedstock. Hence, the biodiesel production cost could be effectively reduced to 60–70 % by using this low raw material.[9,10]

The transesterification is performed in the presence of a suitable catalyst in order to obtain reasonable conversion of triglyceride to biodiesel (Fig. 1). Homogeneous catalysts (acidic: H_2SO_4 and H_3PO_4 or basic: NaOH and KOH) are commonly applied in the transesterification of Jatropha oil.[9,11] The main obstacles to homogeneous catalysts are difficult to recover and lead to downstream waste treatment, increasing the biodiesel production cost.[12] Heterogeneous catalysts have been studied for producing biodiesel from jatropha oil. Soares Dias and co-workers[13] reported that biodiesel production from soybean oil using cerium modified solid basic magnesium alumina (Mg/Al) catalyst showed FAME

yield of > 90 %. Moreover, Margandan *et al.*[14] investigated the catalytic activity of cerium oxide (CeO_2) impregnated alkali zeolite (NaZSM-5) catalyst in transesterification of Jatropha oil with methanol. The result exhibited that CeO_2/NaZSM-5 catalyst showed highly activity (90 % biodiesel yield). However, it required high reaction temperature of 100 °C to achieve the high conversion.

Calcium-based catalysts are solid base catalyst widely investigated in the transesterification because they are cheap and have superior performance at a very low reaction temperature. Zhu *et al.*[15] used calcium oxide (CaO) to catalyze the transesterification reaction of jatropha oil with methanol yielded 93 % of biodiesel. However, bulk CaO is low surface area and not efficient to contact reagent abundantly. Moreover, the leaching of Ca^{2+} ion species into reaction media contaminated the biodiesel product and reduced catalyst service lifetime.

The activity and stability of CaO can be improved by mixed with other metal oxides, such as MgO[6], La_2O_3[8,17] and CeO_2.[16,17] Among the mixed metal oxides, CaO mixed CeO2 catalyst revealed good catalytic activity in biodiesel industry. CaO-CeO_2 catalyst has been reported for producing biodiesel from edible grade refined palm[16] and soybean[17] oils, respectively. Thitsartarn and Kawi[16] reported CaO-CeO_2 catalyst synthesized by sol gel with co-precipitation method. The sol gel process included precipitation of metal ions with ammonia aqueous solution at a constant pH value to form white colour of gel-liked solution. However, sol gel process is more time consuming and need to maintain complicated preparation steps. CaO-CeO_2 catalyst was tested for methanolysis of palm oil, which showed good performance (>10 reaction cycles) during transesterification reaction. Nevertheless, there were some homogeneous species leaching out from the catalyst into biodiesel product. High concentration of leached Ca (102 ppm) and Ce (57 ppm) species were observed in biodiesel product.

To best of our knowledge, no report on catalytic performance of $CaO-CeO_2$ mixed oxides for transesterification of non-edible crude *Jatropha curcus* oil (JCO) has been investigated. A series $CaO-CeO_2$ mixed oxide catalysts were currently prepared by simple co-precipitation method to improve the interaction of catalyst components in bimetallic system. This catalyst was used as an active and stable catalyst for the production of a clean and green alternative fuel. Physico-chemical properties of mixed oxide catalysts were characterized and discussed. The effect of Ca-to-Ce molar ratio on the catalytic activity and leaching behaviour of $CaO-CeO_2$ mixed metal oxide catalysts for transesterification of crude JCO were determined. Lastly, a screening of the reaction conditions (*i.e.* methanol/ oil molar ratio, catalyst concentration and reaction time) and reusability of catalyst for transesterification reaction has also been performed.

Results and discussion

Crude JCO characteristics

The physicochemical properties of crude JCO were revealed in Table 1.[18,19] Acid value (AV) of crude JCO was 13.6 mg KOH g^{-1} whereas it had 6.8 % (as oleic) of free fatty acid (FFA). The density and saponification values of crude JCO were 0.92 g cm^{-3} and 188.40 mg KOH g^{-1}, respectively. Therefore, the average molecular weight of crude JCO was calculated as 962.8 g mol^{-1}.

TG/DTA studies

Fig. 2 showed the TG/ DTA curves of the catalyst precursor before calcination. The DTA peaks closely corresponding to the weight changes observed on TGA curves. The total mass loss from 50–750 °C was found to be 18.1 %. All curves indicated that decomposition mainly occurred via two distinct stages and was complete at about 800 °C. The weight loss found from TGA measurements agree fairly well with those expected for decomposition of

hydroxycarbonates ($M_2CO_3(OH)_2$) to different oxides of calcium and cerium. According to the following thermal decomposition equation (Eq. 3), the first state of mass loss from 50–150 °C associated with the structural water loss was 6.9 %.

$$CeO_2 \cdot 2H_2O \rightarrow CeO_2 + 2H_2O \text{ (vapor)} \quad (3)$$

$Ce(OH)_4$ is a hydrous oxide, represented by $CeO_2 \cdot xH_2O$ which dehydrates progressively. Therefore, the decomposition of precursor is a form of dehydration process of the hydrated CeO_2. It was suggested that the precipitate consisted of a mixture of phases such as $CeO_2 \cdot 2H_2O + CeO_2$.[20] Besides, weight loss below 100 °C could be due to absorbed moisture. The final weight loss (11.2 %) at 550–750 °C signified the decomposed of $M_2CO_3(OH)_2$.[20]

Structure and crystallography

Fig. 3(a) and 3(b) depict the powder XRD patterns of the CeO_2, CaO and CaO-CeO_2 catalysts produced with different preparation variables (pH and Ca/Ce molar ratio). The pure CaO gave well defined and narrowed crystalline diffraction peaks at 2θ value of 32.1°, 37.2°, 53.9°, 64.0° and 67.2° (JPDS File No. 00-037-1497) corresponding to the presence of cubic crystal structure associated with reflections from (110), (200), (220), (311), (222) and (400) planes, respectively. The fluorite type cubic structure of pure CeO showed the characteristic reflections at 2θ value of 28.5°, 33.1°, 47.5°, 56.4°, 59.2°, 69.6, 76.9° and 79.3° from (111), (200), (220), (311), (222), (440), (331) and (420) planes, respectively. CaO-CeO_2 mixed oxide catalysts (Fig. 3) gave the formation of cubic CaO and fluorite type cubic CeO_2 phases in binary metal system. The XRD analysis of these co-precipitated CaO-CeO_2 catalysts revealed characteristic peaks of its separated metal oxide crystalline phases without the presence of any new formation of mixed oxide phases (homogeneous CaO-CeO_2 mixed solid solutions) could be detected in the precipitate particles. This was mainly due to the different ionic radii of the metal ions.[7] In Fig. 3(a), the increased in pH synthesis (9~12) resulted in an increased and a decreased in peak intensities of CaO and CeO_2, respectively. On the other

hand, addition of CaO to CeO_2 matrix was resulted in an insignificant change in XRD patterns (Fig. 3(b)) of CeO_2. The peak intensity of the CaO phase was found to be low whereas a strong reflection associated with fluorite type cubic structure of CeO_2 was observed in the XRD profile. With increased in the Ca/Ce molar ratio, the XRD peaks associated with the cubic CaO phase become more intense, and concomitantly those of CeO_2 decreases significantly. This can be attributed to the higher X-ray scattering factor of Ca^{2+} compared to the Ce^{4+} ions.[21]

Moreover, the dependence of CeO_2 mean crystallite sizes as measured by XRD on the calcium concentration from 0.25–19.0 Ca/Ce molar ratio were presented in Table 3. The pure oxides exhibited the metal CaO and CeO_2 clusters with 66.3 and 48.6 nm in mean crystalline size, respectively, decreased to become 54.2 and 39.2 nm for binary oxide CaCe0.25. Nevertheless, the decrease seems to reach a threshold from a Ca/Ce molar ratio of 0.67. Above Ca/Ce molar ratio of 0.67, the decreased of CaO and CeO_2 crystalline sizes become less pronounced and it was increased in crystalline sizes until 75.8 and 49.7 nm for CaCe19.0. Initially, the addition of calcium component into CeO_2 crystalline structure at low concentration was first located between the CeO_2 grain boundaries and thus disturbs the normal growth of the CeO_2 crystallites at high concentration.[20] This indicated that the CeO_2 mean crystalline size increased linearly with the loading of calcium content (Fig. 4) from low to high concentration. This result demonstrated that the volume of the CeO_2 cell has increased due to the Ca^{2+} effective ionic radius (1.12 Å), which is larger than that of Ce^{4+} (0.97 Å).[20] The results indicated that crystal sizes of catalysts were in agreement with the line width of the peak in which decrease of FWHM with the increment of the crystallite size. It was also suggested that the high dispersion of CaO on the composite give rise to low crystalline size for CaCe0.25. However, agglomeration and sintering effect of particle size to

form bulk particles resulting from overloading of secondary metal and high calcinations temperature could be occurred at above Ca/Ce molar ratio of 0.67.[2,3,5,7,8]

Catalyst composition and surface area

Tables 2 and 3 demonstrated the efficiency of CaO-CeO_2 catalysts synthesized through different preparation variables (pH and Ca/Ce molar ratio) by evaluated the catalyst compositions. As mentioned above, only the CaO-CeO_2 (CaCe4.00-11 and CaCe4.00-12) catalysts (Table 2) synthesized at pH 11 and 12 indicated high content of CaO in the composites with Ca/Ce molar ratios at 4.39 and 3.53, respectively. Besides, Ca/Ce atomic ratios were found in the precipitated solids closed to the theoretical ratios at pH 11–12. This phenomenon was due to the fact of Ca^{2+} ion is favourably to precipitate at relative high pH value (pH 11). However, Ce^{4+} ion is readily solidified or more soluble at high pH value of pH 12.[7,8] From Table 3, the Ca/Ce molar ratio of the catalyst decreased when CeO_2 content increased. In addition, the BET surface area of CaO-CeO_2 mixed oxide catalysts with different Ca/Ce molar ratios were presence in Table 3. The bulk CaO and CeO_2 exhibited high and low surface area of 52.6 and 9.2 m^2g^{-1}. The surface area of the CaO-CeO_2 mixed oxide catalysts was in agreement with XRD analysis which showed that larger crystallite sizes gave lower surface area (Fig. 4).[17,20] The surface areas increased with added of CeO_2, suggesting that CeO_2 was incorporated with the CaO and both was well dispersed on the catalyst surfaces as shown in (Fig. 7(ii)). Besides, it is well known that an increased in surface area of catalyst might favourable for improving the catalytic performance. Conversely, the low FAME yield (40 %) observed at CaCe0.25, which might be related the change of active sites on the catalyst surface due to addition of low CeO_2 content. The surface area of the catalysts (CaCe0.67 to CaCe19.0) decreased when calcium loading increased (Table 3). The overloading of the CaO particle on the surface or into the porous structure of CeO_2 that cause saturation or filling of pores in catalyst composition also

contributed to the reduction of CaO-CeO_2 catalyst surface area.[8] Furthermore, the decrement in surface area may also due to high calcination temperature (900 °C) that lead to sintering effect on fine crystal and promoted cluster agglomeration.[8]

Surface functional group

FTIR spectra of CaO, CeO_2 and CaO-CeO_2 catalysts were shown in Fig. 5. All spectra present a large absorption band located at around 500 cm^{-1}, which attributed to the Ca-O, Ce-O and Ca-O-Ce stretching vibration.[20] Besides, the band located at around 1799 cm^{-1} corresponded to the H-O-H bending vibration, indicated the presence of moisture absorbed after calcinations process.[20] In the previous studies, the bands were found at around 711 and 873 cm^{-1} have been attributed to the CO_2 asymmetric stretching vibration and CO_3^{2-} bending vibration, respectively.[21] Both bands were also related to the presence of atmospheric CO_2 on metallic cations[20] and the formation of "carbonate-like" species on the particles surface[21] during the synthesis. Furthermore, another strong intensity band at around 1407 cm^{-1} which was the characteristic vibration mode of isolated CeO_2.[22]

Basicity

The total basicity of CaO-CeO_2 catalysts was evaluated using temperature programmed desorption of CO_2. The TPD-CO_2 profile of CaO-CeO_2 catalysts was revealed in Table 4 and Fig. 6. All mixed oxide catalysts exhibited a high amount of CO_2 desorption peaks, with peaks maxima at 813, 788, 778, 769 and 746 °C, corresponding to basic sites of high strength. The strong basic sites of CaO-CeO_2 catalysts showed the existence of oxygen of Ca-O, Ce-O_2 ion pairs and isolated O^{2-} anions, that can be expected to posses Lewis base character.[8,14] The active sites of the oxide surface may will form an interaction with the proton of methanol and contribute to the breaking of OH bond hence cause the formation of active methanol ion to initiate the transesterification reaction. Basically, the basicity of CaO-

CeO_2 bimetallic an oxide catalyst was found higher than bulk CaO and CeO_2. The order of basicity was found to be as follow: CaCe1.00 > CaCe4.00 > CaCe19.0 > CaCe0.67 > CaCe0.25 > CaO > CeO_2. The improved basicity of bimetallic oxide was due to the synergetic effect between metallic ions of CaO and CeO_2. However, the CO_2 desorption peak moved toward lower temperature for bimetallic oxide catalysts with introduction of more Ca^{2+} (Ca/Ce molar ratio of 0.25–19.0) to the binary oxide, which indicated that the presence of secondary metal phases (CaO) in CeO_2 indeed reduces slightly the basic strength of the catalyst.

Morphology

The morphologies of the catalysts were observed by SEM (Fig. 7). A compact and evenly distributed globular granule was found in pure CaO (Fig. 7(i)) whereas pure CeO_2 (Fig. 7(viii)) particles were mostly fluorite structure with a large size distribution. All CaO–CeO_2 mixed oxide catalysts (Fig. 7(ii) to 7(vii)) were in the form of agglomerated particles of irregular-shaped crystalline particles. The particle size increases substantially with an increase in Ca/Ce molar ratio, indicating an obvious agglomerate of crystallinity. The mixed metal oxide catalyst with agglomeration was in agreement with morphology that has been reported previous for CeO_2-CaO nanocomposite oxide.[23] Numerous macropores were found to be present on surface of the particles (Fig. 7(ii)), which is due to the well dispersion of CaO on the surface and into porous of CeO_2. However, with decreased in calcium content the catalysts become decreasingly porous. In addition, the SEM image indicated that the catalyst morphology was closely related to the high calcination temperature (900 °C). As shown, the CaCe1.00 (Fig. 7(iii)) has a homogeneous agglomeration with smaller particles, which is associated with the better catalytic performance. Nevertheless, mixed oxide catalysts (CaCe4.00 and CaCe19.0) (Fig. 7(vi) and 7(vii)) have rough and disproportionate agglomerate. The big aggregation and sintering effect of the catalyst's particle is also

considered as one of the reasons why the catalyst (CaCe4.00 and CaCe19.0) has a lower surface area.

Optimization of process parameters

Effect of the Precipitation Condition (pH) on the FAME Yield

To investigate the effect of a range of CaO-CeO_2 mixed oxide (CaCe4.00) catalysts prepared via variable pH (9–12) value conditions at the precursor stage upon the molar ratio of each metal component in these catalysts. The concentrations of metal component presence in the catalyst composite were depended on the precipitation pH and subsequently influence the activity of the final calcined catalysts. Table 2 shows the optimum pH preparation conditions were identified with respect to the catalytic activity for transesterification of crude JCO to biodiesel. The CaCe4.00-9 and CaCe4.00-10 catalysts revealed poor catalytic performance due to low precipitate Ca/Ce molar ratio. The result demonstrated that CeO_2 in the catalyst composite is more abundant and it provided low basicity, which is not sufficient for performing complete transesterification reaction.[7,15] The CaCe4.00-11 catalyst showed a significant improvement of the FAME yield with 86.53 % due to increase of the precipitate Ca/Ce molar ratio closed to the theoretical molar ratio. The CaCe4.00-11 catalyst with Ca/Ce molar ratio of 4.39 indicated high content of Ca and Ce in the bimetallic oxide, which provided more active basic sites for transesterification process. With further increased of pH preparation, reduced the FAME yield production from CaCe4.00-12 catalyst.

Effect of the Ca/Ce molar ratio of catalyst on the FAME yield correlation to the basicity of mixed oxide catalysts

CaO-CeO_2 mixed oxide catalysts with different Ca/Ce molar ratio were screened for the transesterification activity on crude JCO, which indicated in Fig. 8. The transesterification was evaluated with crude JCO-to-methanol ratio of 1:12 at 65 °C with 4 wt. % catalyst (with

respect to the weight of oil). The results showed that Ca/Ce molar ratio was greatly affected to the biodiesel yield production. The FAME yield of CaCe0.67, CaCe1.00, CaCe4.00 and CaCe19.0 catalysts were higher than CaCe0.25 catalyst. The catalyst with high CeO_2 content, exhibited low production of FAME. When the Ca/Ce molar ratio increased from 0.25 to 0.67, the FAME yield increased remarkable from 40.61% to 80.59 %, respectively. Further increment of Ca/Ce molar ratio to CaCe1.00 resulted the maximum yield of FAME. Unfortunately, a significant dropped in catalytic activity was observed at beyond a Ca/Ce molar ratio of 4 and 19. Previous studies showed that transesterification activity dependence on the amount of basic sites of the catalyst.[7,8] The results of CO_2-TPD supported the finding as shown in Fig. 6 and summarized in Table 4. The increased in FAME yield from 40 to 87 % with increment of Ca content from CaCe0.25 to CaCe1.00 is due to the increment of basicity from 2.81 to 8.20 (x 10^{-3} mol g^{-1}). The co-relationship between basicity and activity of the catalyst was demonstrated in Fig. 8. The improve basicity of CaO-CeO_2 mixed oxide catalyst was due to the synergetic effect between metallic ions of CaO and CeO_2. Nonetheless, a tremendous amount of catalyst components was observed to leach out from catalysts into the reaction media during the reaction.

The dissolution homogeneous species are known to be involved in the catalysis of the reaction.[17] The reaction parameters *i.e.* catalyst amount, 4 wt. %; (methanol):(oil) ratio, 12:1; reaction temperature, 65 °C and reaction time, 6 h were tested. As illustrated in Fig. 8, bulk CaO exhibited both the highest FAME yield of 90 % and the highest contribution of homogeneous catalysis (FAME yield of 32 %). These results indicated that pure CaO can easily dissolved into the polar phase (methanol) and form calcium methoxide species as the homogeneous catalyst. Hence, the biodiesel yield was due to the superior mass transfer for this homogeneous catalyst. For mixed metal oxide catalysts, when the Ca/Ce molar ratio increased to 0.25, a concomitantly remarkable decreased in homogeneous contribution to 0.4

% FAME yield was also observed. Furthermore, the low FAME yield was demonstrated from reaction catalyzed by methanol solution containing the active homogeneous species leaching out from CaCe0.67, CaCe1.00 and CaCe4.00 catalysts and the high FAME yield was obtained from CaCe19.0, respectively. The results indicated that the homogeneous species leaching out from solid catalysts into the methanol solution are actively involved in the reaction.

Therefore, the good catalytic performance of CaCe0.67, CaCe1.00, Cace4.00 and CaCe19.0 catalysts was mainly attributed to the solid basic sites of the catalyst with a very low homogeneous behaviour. However, the reasonable Ca/Ce molar ratio for transesterification of crude JCO to FAME is CaCe1.00. By correlation of this tendency with the increased and decreased peak intensity of CaO and CeO_2 phases shown at XRD patterns, it can be inferred that an interaction between the surface CaO and the CeO_2 most likely exists. Soares Dias *et al.*[13] reported that over 90 % of methyl ester yield obtained with catalyzed soybean oil with Ce/Mg/Al catalyst. The used of tri-metal catalyst system increased the cost production of biodiesel. On the other hand, the leaching of Ce^{2+}, Mg^{2+} and Al^{3+} ions into product still remained unknown.

Effect of molar ratio of methanol/oil on FAME yield

The molar ratio of methanol to crude JCO was varied from 9:1 to 24:1 (Fig. 9). The yield of FAME for transesterification of crude JCO increased in the methanol/oil molar ratio up to 15:1, which achieved the maximum ester yield of 95.59 %. With further increase in methanol/oil molar ratio to 18:1, the change in the yield was insignificant. However, the FAME yield was decreased considerably to 82.94 and 74.22 % at methanol molar ratio of 21:1 and 24:1, respectively. The results showed that a higher methanol/oil molar ratio is required to get better conversion. Nonetheless, an excess of polar OH group from methanol will cause emulsification that interfere in the separation of as-synthesized and glycerine as

more energy required to recover it. Moreover, it can increase the dissolution of oil, intermediates and biodiesel product in a high volume of methanol, which resulting in the wastage of the raw reactants. Therefore, 15:1 is the appropriate methanol/oil molar ratio for this reaction. Previously, it was found that transesterification of palm oil required more methanol-to-oil molar ratio which is 20:1 to achieve high FAME yield production with CaO-CeO_2 catalyst prepared by Thitsartarn and Kawi.[16]

Effect of the catalyst dosage on FAME yield

Fig. 10 depicted the influence of the catalyst amount on biodiesel yield. The catalyst amount was varied in range of 1–6 wt. % (with respect to the oil weight). The FAME yield (24 %) was initially quite low at less quantity of catalyst amount of 1 wt. %. The yield appeared to increase with an increase in catalyst amount due to an increase in the number of active sites. The maximum FAME yield of 95.57 % was obtained at 4 wt. % catalyst dosage. However, a slight reduced in yield was found at catalyst concentration at above 2 wt. %. This effect was attributed to the poor diffusion between the methanol–oil–catalyst systems in this case.[4,8,11] Kim *et al.*[17] stated that the FAME yield of 91 % were recorded with 8 wt.% of CaO-La_2O_3 supported on CeO_2 catalysts. Nevertheless, it should be noted that Kim *et al.*[17] used transition supported metal oxides *i.e.* La_2O_3 and CeO as catalyst in relatively high concentration, which is increased the biodiesel production cost.

Effect of the reaction time on FAME yield

The dependence of the FAME yield on the reaction time was studied. As demonstrated in Fig. 11, the reaction time effect on the FAME yield was investigated in range of 2–10 h. Initially, the FAME yield of 36.99 % was reached at short reaction time (2 h). This was due to the limitation of solid mass transfer that caused poor mixing and dispersion of the solid reactant. However, the conversion for the catalyst was increased gradually after 2 h of

reaction time. The nearly equilibrium FAME yield was found to be around 95 % at 6 h of reaction time. With further prolongation of reaction time beyond 6 h was dramatically reduced the FAME yield to 70 % due to the reverse transesterification process.[7]

Catalyst stability

Fig. 13 presents the reusability study of CaCe1.00 for transesterification of crude JCO under the best reaction conditions (10 g of oil, methanol/oil molar ratio of 15;1, catalyst amount of 4 wt. % and reaction temperature of 65 °C). After each cycle of 6 h of the reaction, the catalyst was separated, washed several times with methanol and *n*-heptane. The resultant dried solid particles were calcined at 900 °C for 3 h and simultaneously reused in new batch transesterification process. The FAME yield decreased slowly from 97.57 to 83.41 % when this process was repeated 1–4 times. On the other hand, a significant loss in catalytic performance was observed in 5th run, which indicated a remarkable reduction of the number of active sites on the catalyst surface after a numerous times washing and recalcination processes.[16,17] The two possibility reasons behind catalyst deactivation *i.e.* surface poisoning and structure collapsing.[5,7,8] The surface poisoning might be due to the surface bound glycerides, *i.e.* triglycerides (TG), diglyceride (DG) and monoglyceride (MG) on catalyst, which unable to remove with the less polar solvent.[7] These coated materials were inhibited on the active sites of the catalyst. Furthermore, the repeating calcinations process will cause the morphology change and reduced the interaction between CaO and CeO_2.[16,17,20]

The EDS and AAS analysis were carried out to investigate the leaching active species (Ca and Ce) for CaCe1.00 mixed oxide catalyst (fresh and fifth run catalysts) (Fig. 5). EDS analysis for fresh, 1st, 3rd, and 5th run CaCe1.00 catalysts exhibited gradually decreasing in CaCe molar ratio from 1.33 to 0.81, indicated less leaching of active metal in the reaction medium. Hence, it is implicated that the presence of interaction between active phases CaO-CeO_2 binary metal osxide could stabilized active phases of catalyst in order to reduce its

lixiviation to the reaction medium. Besides, the FAME from all reusability cycles was tested using AAS to evaluate the concentration of leached Ca^{2+} and Ce^{4+} ions. The results revealed the insignificant loss of active metal ions in biodiesel product, with concentration of Ca in the range of 5.79–2.49 ppm and 5.51–3.21 ppm of Ce content, respectively. However, these minor leached metal ions were complied with the standard of EN 14214 specification, indicated the produced biodiesel was suitable to be use as vehicle fuel. The concentration of Ca and Ce species decreased significantly in biodiesel with subsequent reaction cycles, and reach about 3–4 ppm after 5th run. The decreased amount of the leached species were attributed to the good interaction between Ca and Ce, which was due to the vacancies created by substitution of Ce^{4+} by Ca^{2+} ions via electron transfer.[16] Since the content of dissolved Ca and Ce species in the reaction medium was very low (3–4 ppm), the FAME yield showed from 5th run onward was mainly contributed by the heterogeneity CaCe1.00 catalyst and not by the homogeneous catalytic species dissolved in the reaction mixture. Therefore, the results of reusability and regeneration definitely indicated that CaCe1.00 mixed oxide catalyst is very stable and durable during transesterification reaction, which is better than that reported by Thitsartarn and Kawi[16].

Experimental

Materials

Commercially crude JCO was obtained from Bionas Sdn Bhd, Malaysia and used without further purification. The reagents cerium (III) nitrate hexahydrate ($Ce(NO_3)_2{\cdot}6H_2O$) (Sigma-Aldrich, 99.9 %), calcium (II) nitrate tetrahydrate ($CaNO_3{\cdot}4H_2O$) (R&M Chemicals, 99.9 %), sodium hydroxide (NaOH) (Merck, 99.0 %), sodium carbonate anhydrous (Na_2CO_3) (Bendosen, 99.0 %) and commercial CaO (SigmaAldris, 99.0 %). Anhydrous methanol (Merck, 99.7%) and dichloromethene (Merck, 99.7 %) were purchased from Fisher Scientific. Analytical reagent grades were applied throughout the experimental. The

properties of crude JCO were identified from the data obtained using Malaysia Palm Oil Board (MPOB) standard methods. So, the average molecular weight (M) of crude JCO was calculated with the following equation[8] as following (Eq. 1):

$$\mathrm{M} = \frac{56.1 \times 1000 \times 3}{\mathrm{SV} - \mathrm{AV}} \quad (1)$$

where, AV is the acid value and SV is the saponification value of crude JCO.

Catalyst preparation

$CaO\text{-}CeO_2$ mixed oxides were prepared according to the co-precipitation method and follows calcinations of the precursors. In a typical synthesis, a mixture of nitrate salts of $CaNO_3{\cdot}4H_2O$ and $Ce(NO_3)_2{\cdot}6H_2O$ were dissolved in calculated quantity of deionizer water. The two precursor were mixed homogeneously and allow to precipitate using super base solution of NaOH (0.04 mol) and Na_2CO_3 (0.01 mol) at a constant pH. The resulted suspension was stirred at 65 °C for 24 h. The solid product was recovered by filtration, followed thorough washing with deionized water and drying in an oven at 110 °C overnight. The dried solid was calcined at 900 °C for 6 h with the ramp at 5 °C min^{-1}. The $CaO\text{-}CeO_2$ mixed oxide catalysts were reffered to as CaCe*x*-*y* in the subsequent text where *x* represents the Ca/Ce molar ratio and *y* is the pH value of preparation method.

Catalysts characterization

Thermogravimetric

Thermogravimetric and differential thermal analysis (TG/DTA) was employed on a Mettler Toledo thermogravimetric analyzer. These tests were performed under a continuous nitrogen flow (100 ml min^{-1}) over a temperature range of 35–1000 °C at a heating rate of 10 °C min^{-1}.

Structure and crystallography

The powder X-ray diffraction (XRD) analysis was performed with a XRD6000 powder X-ray diffractometer (Shimadzu Corporation, Japan) at ambient temperature. The Cu Kα radiation was generated by a Philips glass diffraction X-ray tube (broad focus 2.7 kW type), with a step size of 0.04° in the 2θ range from 10 to 80°, was used to generate diffraction patterns from the powder crystalline samples. The data was processed with the X'Pert High Score Plus software. The peaks were identified using the Powder Diffraction File (PDF) database created by International Centre for Diffraction Data (ICDD). Then, the crystallite size of the powder catalysts was calculated with Debye-Scherer's equation.[8]

Elemental analysis

The real molar ratio of catalyst components (Ca/Ce) was determined by energy dispersive X-ray fluorescence (XRF) spectrometer using Bruker AXS. The measurements were performed using calibration curves based on the XRF measurements for the prepared mixtures from silica (Degussa). The metal concentration in the examined samples was determined by the amount of emitted X-ray radiation related to the values in the calibration curves.

Surface functional group

Infrared spectra (IR) were conducted on a Perkin Elmer (PC) Spectrum 100 FTIR spectrometer using attenuated total reflection-Fourier transform-infrared (ATR-FTIR), to identified the surface functional group of catalyst, over the wave number range of 650–4000 cm^{-1}, with 4 cm^{-1} resolution. All measurements were conducted at room temperature.

Specific surface area

The total surface area of the catalysts was carried out using the Brunauer- Emmer-Teller (BET) method, with corresponding to the multi point N_2 adsorption-desorption isotherms at -

196 °C. The analysis was conducted using a Micromeritics ASAP-2020. Prior to measurements, all catalysts were out-degassed for 8 h at 200 °C.

Basicity

The basicity were evaluated by using temperature programmed desorption method with CO_2 as probe molecule (CO_2-TPD). These experiments were carried out using a Thermo Finnigan TPD/R/O 1100 series apparatus equipped with a thermal conductivity detector (TCD). In a typical experiment approximately 0.1 g of catalyst was pre-treated in an N_2 gas flow (30 ml min^{-1}) at 500 ◦C for 1 h. Subsequently the catalyst was brought to room temperature and saturated with CO_2 gas. Desorption of carbon dioxide was performed after flushing using carrier gas over a temperature range of 30–900 °C at a heating rate of 10 °C min^{-1}.

Morphology

The surface structure and element composition of catalyst was observed from a Hitachi s-3400 scanning electron microscopy coupled with energy dispersive X-ray detector (SEM-EDX) spectroscopic at room temperature. The catalysts were coated with gold using a Sputter Coater and accelerating voltage was 20 KV. The element composition was analyzed by using an EDS detector mounted on the microscope.

Catalytic activity and biodiesel analysis

The transesterification reactions were carried out by mixing crude JCO, catalyst and methanol in a 250 ml two necked reaction flask. The reactor was magnetically stirred and equipped with a condenser, a thermometer, and a heating mantle. Unless otherwise noted, catalytic activity tests will perform in the presence of 4 wt. % catalyst, a methanol/oil ratio of 12:1, and a reaction temperature of 65 °C for 6 h. At the end of the experiment, the catalyst was separated from the mixture by centrifuged and the mixture was then loaded into rotary evaporator to remove excess methanol. After the methanol evaporation, the liquid phase

(biodiesel and glycerol) was dissolved in hexane and then washed with hot distilled water for several times for refinement. The moisture of the washed biodiesel was subsequently removed using anhydrous magnesium sulphate. Finally, the liquid phase was kept in separating funnel to separate the lower glycerol layer from upper FAME layer. The glycerol was could be separated because it was insoluble in the esters and had a much higher density.

The quantification and qualityfication of biodiesel (FAME) were measured using a Shimazu GC-14C Gas Chromatograph System equipped with a flame-ionization detector (FID), a split/splitless injector and a polar BP-20 capillary column (30 m x 0.5 mm x 0.25 μm) with helium as the carrier gas and a flow rate of 1.5 ml min^{-1}. Ester contain was quantified according to EN 14103[7] in the presence of methyl heptadecanoate ($C_{18}H_{36}O_2$) as an internal standard. The analysis of biodiesel for each sample was carried out by dissolving 1g of biodiesel sample into 10 ml of *n*-hexane and injecting 0.1 ml of this solution for each injection. The amount of FAME was calculated and expressed as mass fraction in percentage using the following equation (Eq. 2):

$$\text{FAME yield (\%)} = \frac{\Sigma \text{A} \times A_{\text{IS}}}{A_{\text{IS}}} \times \frac{C_{\text{IS}} \times V_{\text{IS}}}{m} \times 100 \qquad (2)$$

where ΣA is the total peak area of JCO fatty acid methyl esters with carbon numbers C16–20 with unsaturated 0–2; A_{IS} is the internal standard peak area; C_{IS} is the concentration of the internal standard solution in mg ml^{-1}; V_{IS} is the volume of the internal standard solution used in ml; m is the mass of sample in mg. Each experiment was conducted in triplicate and the data reported as mean ± standard deviation.

Catalyst stability

To evaluate stability of the $CaO\text{-}CeO_2$ catalysts, leachate test was conducted by mixing catalyst ($CaO\text{-}CeO_2$ catalysts with different Ca/Ce molar ratios) with methanol, under the same conditions as used in the transesterification process without oil presence. After that, the

catalyst was separated, and remaining methanol solution was reacted with the necessary volume of fresh crude JCO. The leachate test was performed to evaluate the contribution of homogeneous catalysis originating from the leaching of active sites (Ca^{2+}).

In addition, the recycle use of catalyst was performed to study the reusability. After completion of each run, the use catalyst was separated from the reaction mixture and washed several times with methanol and n-heptane solvents simultaneously to remove the surface bound glycerides, *i.e.* triglycerides (TG), diglyceride (DG) and monoglyceride (MG) from the catalyst. The resultant solid particles were treated at 900 °C for 3 h and used for further recycling studies.

Conclusions

The CaO-CeO_2 mixed oxide catalysts prepared by super alkaline co-precipitation method were successfully used for transesterification of crude JCO to biodiesel. The activity and stability of CaO-CeO_2 mixed oxide catalysts were greatly influenced by pH synthesis and Ca/Ce molar ratio. Among these CaO–CeO_2 catalysts, CaCe1.00 (which comprised of a Ca/Ce molar ratio of 1 and calcined at 900 °C) catalyst has superior catalytic performance for transesterification as it showed the highest BET surface area and total basicity. Under the optimized conditions at 65 °C, 4 % catalyst dose with a 24:1 molar ratio of methanol to *Jatropha* oil, the catalyst exhibited 95.57 % of biodiesel yield. CaCe1.00 catalyst also revealed a low leaching of homogeneous catalytic species (*i.e.* Ca and Ce) into the reaction media. Less Ca^{2+} and Ce^{4+} ions of around 3–4 ppm was showed that the dissolved metal species from calcium-based mixed oxides into reaction medium is insignificant, which is lower than the standard limit according to biodiesel quality standards. In addition, the catalyst could be reused for 4 times with good performance (> 90 % FAME yield). The bimetallic oxide system improved the heterogeneous catalytic stability remarkably due to the defects induced by substitution of Ca ions for Ce ions on the surface. The result clearly suggests that

the CaCe1.00 catalyst is very stable and durable during transesterification reaction and the contamination of the catalyst component in the biodiesel product is no longer a problem for the long-term usage of this catalyst.

References

1 M. K. Lam, K. T. Lee, A. R. Mohamed, *Biotechnol. Adv.*, 2010, **28(4)**, 500.

2 J. C. Juan, D. A. Kartika, T. Y. Wu, Y. H. Taufiq-Yap, *Bioresour Tech.*, 2010, **102**, 452.

3 Y. H. Taufiq-Yap, S. Sivasangar, A. Salmiaton, *Energy*, 2012, **47(1)**, 158.

4 H. T. Tan, K. T. Lee, A. R. Mohamed, *Bioresour. Technol.*, 2010, 101, 5719.

5 A. Islam, Y. H. Taufiq-Yap, C. M. Chu, E. S. Chan, P. Ravindra, *Process Saf. Environ.*, 2013, **91**, 131.

6 F. Muhammad, R. Anita, S. Duvvuri, *J. Clean Prod.*, 2013, **59**, 131.

7 H. V. Lee, R. Yunus, J. C. Juan, Y. H. Taufiq-Yap, *Fuel Process. Technol.*, 2011, **92**, 2420.

8 Y. H. Taufiq-Yap, S. H. Teo, U. Rashid, A. Islam, M. Z. Hussien, *Energy Convers. Manage.*, 2014. http://dx.doi.org/10.1016/j.enconman.2013.12.075

9 M. M. Gui, K. T. Lee, S. Bhatia, Energy 2008, **33**, 1646.

10 K. E. Abebe, K. Yohannes, Z. Rolando, *Energy.*, 2011, **36**, 2693.

11 P. D. Patil, V. Gnaneswar, S. G. Deng, *Ind. Eng. Chem. Res.*, 2009, **48**, 10850.

12 S. Tamalampudi, M. R. Talukder, S. Hama, T. Numata, A. Kondo, H. Fukuda, *Biochem. Eng. J.*, 2008, **39**, 185.

13 A. P. Soares Dias, J. Bernardo, P. Felizardo, M. J. Neiva Correia, *Energy*, 2012, **41**, 344.

14 B. Margandan, V. Mari, N. G. Andrews, *Bull. Korea Chem. Soc.*, 2013, **34**, 3059.

15 H. Zhu , Z. Wu , Y. Chen , P. Zhang , S. Duan , X. Liu, Z. Mao, *Chin. J. Catal.*, 2006, **27**, 391.

16 W. Thitsartarn, S. Kawi, *Green Chem.*, 2011, **13**, 3423.

17 M. H. Kim, D. M. Craig, S. L. Yan, O. Steven Salley, K. Y. Simon Ng, *Green Chem.*, 2011, **13**, 334.

18 S. A. Raja, D. S. Robinson smart, C. L. Robert Lee, *Res. J. Chem. Sci.*, 2011, **1(1)**, 81.

19 Bionas biofuels: the next generation sustainable energy. Properties of jatropha oil. Available from, http://www.biofuelbionas.com/fuel.html 2014.

20 T. Laurianne, M. T. Ta, D. Thierry, K. Konstantin, H. Valérie, S. Cyriaque, A. Caroline, P. N. Ivan, P. Alain, V. Olivier, J. P. Blondeau, *Mater. Res. Bull.*, 2010, **45**, 527.

21 A. R. West, (2007) Solid State Chemistry and Its Applications, Wiley India Pvt. Ltd.

22 J. K. Jasmine, A. N. Samson, *J. Ceram. Process. Res.*, 2011, **12(1)**, 74.

23 S. Samantary , D. K. Pradhan, G. Hota, B. G. Mishra, *J. Chem. Eng.*, 2012, **193–194**, 1.

Table 1 Physicochemical properties and characteristic of crude JCO

Properties (unit)	[a] Values	[b] Values	[c] Values
Flash point (°C)	214	235	-
Pour point (°C)	6	8	-
Cloud point (°C)	11	2	-
Viscosity at 40 °C (cSt)	36.92	54.8	-
Specific gravity at 29 °C (g cm^{-3})	0.792	0.914	-
Density at 15°C (g cm^{-3})	0.92		0.92 ± 0.15
Water content (%, w/w)	-	0.052	0.09 ± 0.01
Acid value (mg KOH g^{-1})	38.2	0.92-10.0	13.60 ± 0.75
Free fatty acid (as oleic, %, w/w)	-	9.0-12.0	6.80 ± 0.91
Saponification number (mg KOH g^{-1})	195.0	186.5-193.3	188.40 ± 3.10
Fatty acid composition (%)			
Palmitic acid (C16:0)	4.2	13.8	20.2 ± 0.56 [d]
Palmitoleic acid (C16:1)	-	-	1.10 ± 0.05 [d]
Stearic acid (C18:0)	6.9	6.8	7.20 ± 0.91 [d]
Oleic acid (C18:1) (n-9)	43.1	41.7	39.8 ± 0.64 [d]
Linoleic acid (C18:2)	34.3	35.6	31.2 ± 0.41 [d]
Linolenic acid (C18:3)	-	-	0.30 ± 0.03 [d]
Arahidic acid (C20:0)	-	-	0.20 ± 0.02 [d]

[a] Adapted from [18].
[b] Adapted from [19].
[c]Analyzed using Malaysia Palm Oil Board (MPOB) standard methods.
[d]Analyzed using Association of Official Analytical Chemist (AOAC) standard methods.

Table 2 Effect of the precipitation condition (pH) on the FAME yield of crude JCO by CaCe4.00-9, CaCe4.00-10, CaCe4.00-11 and CaCe4.00-12 catalysts

Catalysts	[#] Ca/Ce molar ratio		[*] FAME yield (%)
	Theoritical	Precipitate	
CaCe4.00-9	4.00	0.52 ± 0.95	10.33 ± 1.22
CaCe4.00-10	4.00	0.41 ± 0.05	12.61 ± 0.99
CaCe4.00-11	4.00	4.39 ± 0.75	86.53 ± 5.23
CaCe4.00-12	4.00	3.53 ± 1.24	80.21 ± 2.33

[*] Transesterification condition: catalyst dosage 4 %, *n*(methanol):*n*(JCO) =12:1, reaction time 6 h, reaction temperature 65 °C.

[#] Estimated by XRF analysis.

Table 3 Elemental composition and physicochemical properties of CaO, CeO_2 and CaO-CeO_2 mixed metal oxides with various Ca/Ce ratios

Catalyst	[a] Ca/Ce molar ratio		[b] Crystalitite size (nm)		[c] S_{BET} (m^2g^{-1})
	Theoritical	Experimental	CaO	CeO_2	
CaO	-	-	66.3 ± 3.21	-	9.2 ± 1.61
CeO_2	-	-	-	48.6 ± 2.77	52.6 ± 1.77
CaO-CeO_2	0.25	0.28 ± 0.05	54.2 ± 2.82	39.2 ± 2.54	20.5 ± 2.13
	0.67	0.78 ± 0.15	65.4 ± 2.64	39.4 ± 4.29	17.6 ± 1.22
	1.00	1.12 ± 0.27	62.5 ± 4.24	41.9 ± 2.91	12.7 ± 3.41
	4.00	4.39 ± 0.75	69.9 ± 3.39	42.6 ± 2.39	5.5 ± 1.23
	19.0	16.1 ± 2.54	75.8 ± 2.89	49.7 ± 3.26	4.2 ± 1.02

[a] Estimated by XRF spectroscopy.
[b] Determined from XRD patterns using Sherrer's equation.
[c] BET surface area.

Table 4 The basic intensity of CaO, CeO_2 and CaO-CeO_2 mixed metal oxides with various Ca/Ce ratios

Catalysts	Amount of basicity (x 10^{-3} mol g^{-1})	Temperature range (°C)	Peak temperature (°C)
CaO	2.63 ± 0.63	658-879	813
CaCe0.25	2.81 ± 0.12	685-860	813
CaCe0.67	3.57 ± 0.43	690-864	788
CaCe1.00	8.20 ± 0.89	672-891	778
CaCe4.00	4.19 ± 0.21	666-850	769
CaCe19.0	3.73 ± 0.54	648-779	746
CeO_2	0	-	-

Table 5 Durability studies of $CaO-CeO_2$ catalyst

[a] Number of run	[b] Ca/Ce molar ratio		[c] Biodiesel	
	Theoretical	Experimental	Ca (ppm)	Ce (ppm)
Fresh	1.00	1.33 ± 0.57	1.44 ± 0.04	-
1st run	-	0.88 ± 0.06	7.23 ± 1.11	5.51 ± 1.02
3rd run	-	0.87 ± 0.17	4.22 ± 0.23	3.01 ± 0.12
5th run	-	0.81 ± 0.08	3.93 ± 0.79	3.21 ± 0.27

[a] Transesterification condition: reaction temperature of 65 °C, 6 h reaction time, 4 wt.% of catalyst and methanol/oil ratio of 15:1.
[b] Determined by EDS analysis.
[c] Concentration of calcium in biodiesel determined by AAS analysis.

Figure of Captions:

Fig. 1 Biodiesel (fatty acid methyl esters) production by triglycerides transesterification in the presence of catalyst.

Fig. 2 TG/DTA spectrum of CaO-CeO_2 mixed metal oxide.

Fig. 3 X-ray diffraction patterns of (a) CeO_2 (i), CaCe4.00-pH9 (ii), CaCe4.00-pH10 (iii), CaCe4.00-pH11 (iv), CaCe4.00-pH12 (v) and CaO (vi) catalysts; (b) CeO_2 (i), CaCe0.25 (ii), CaCe0.67 (iii), CaCe1.00 (iv), CaCe4.00 (v), CaCe19.0 (vi) and CaO (vii) catalysts. ♣, characteristic peak of CaO and Δ, characteristic peak of CeO_2.

Fig. 4 Crystallites sizes and BET surface area of CaO-CeO_2 mixed metal oxides.

Fig. 5 FTIR spectrum of CaO (i) CeO_2 (ii) and CaO-CeO_2 (iii) catalysts.

Fig. 6 CO_2-Temperature programmed desorption profiles of CeO_2 (i), CaCe0.25 (ii), CaCe0.67 (iii), CaCe1.00 (iv), CaCe4.00 (v), CaCe19.0 (vi) and CaO (vii) catalysts.

Fig. 7 SEM micrographs of CaO (i), CaCe0.25 (ii), CaCe0.67 (iii), CaCe1.00 (iv), CaCe4.00 (v), CaCe19.0 (vi), and CeO_2 (vii) catalysts.

Fig. 8 Catalytic performance of CaO-CeO_2 catalysts with different Ca/Ce molar ratios: (a) using heterogeneous catalyst, (b) using homogeneous species presence in methanol solution and (c) basicity of CaO-CeO_2 catalysts. Transesterification condition: oil= 10 g, *n*(methanol):*n*(oil) = 12:1, catalyst dosage = 4 wt. %, reaction time = 6 h, reaction temperature = 65 °C.

Fig. 9 Effect of methanol/oil ratio on the FAME yield of crude JCO. Reaction condition: oil= 10 g, catalyst dosage = 4 wt. %, reaction time = 6 h, reaction temperature = 65 °C.

Fig. 10 Effect of catalyst loading on the FAME yield of crude JCO. Reaction condition: oil= 10 g, *n*(methanol):*n*(oil) = 15:1, reaction time = 6 h, reaction temperature = 65 °C.

Fig. 11 Effect of reaction time on the FAME yield of crude JCO. Reaction condition: oil= 10 g, *n*(methanol):*n*(oil) = 15:1, catalyst dosage = 4 wt. %, reaction temperature = 65 °C.

Fig. 12 Gas chromatography of (a) standard references of fatty acid methyl esters (1000 ppm) and (b) transesterification of jatropha derived biodiesel (FAME).

Fig. 13 Recyclability study of catalyst [Reaction condition: Oil = 10 g, catalyst dosage = 4 wt. %, (methanol):(oil) = 15:1, reaction time = 6 h].

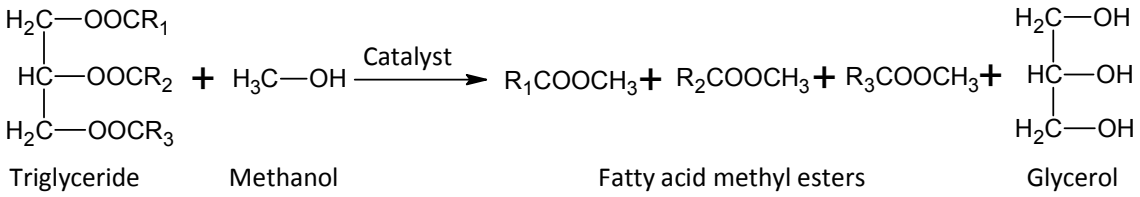

Fig. 1 Biodiesel (fatty acid methyl esters) production by triglycerides transesterification in the presence of catalyst.

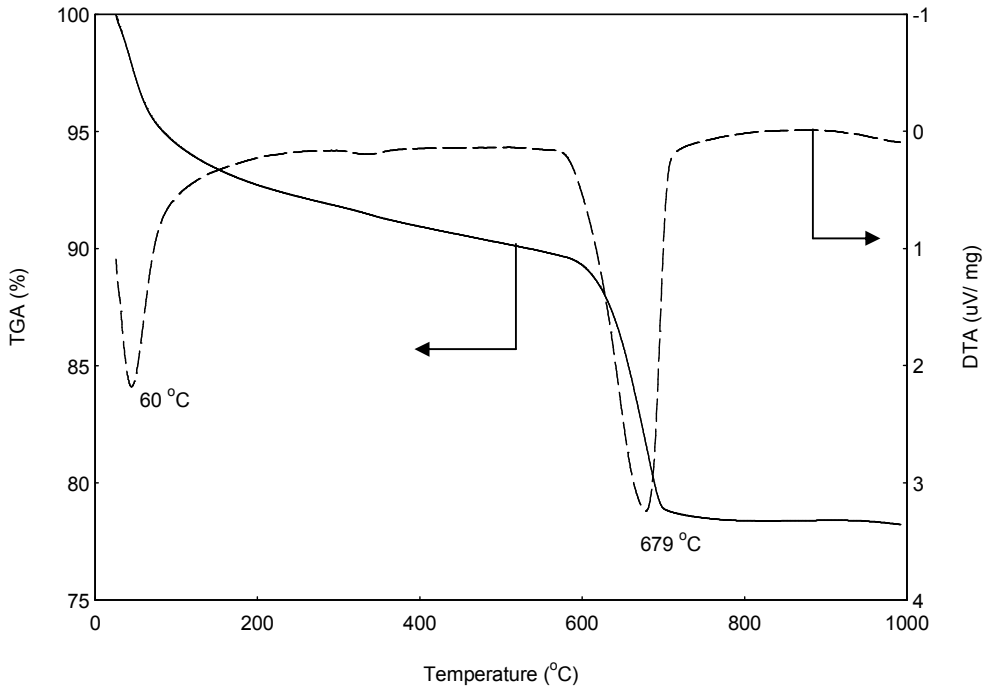

Fig. 2 TG/DTA spectrum of $CaO\text{-}CeO_2$ mixed metal oxide.

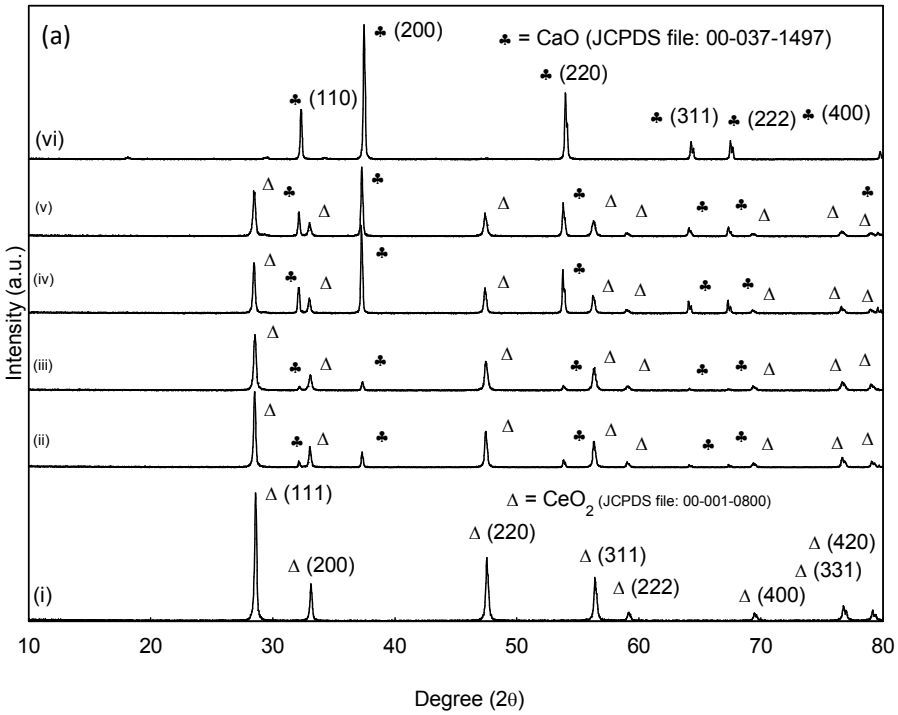

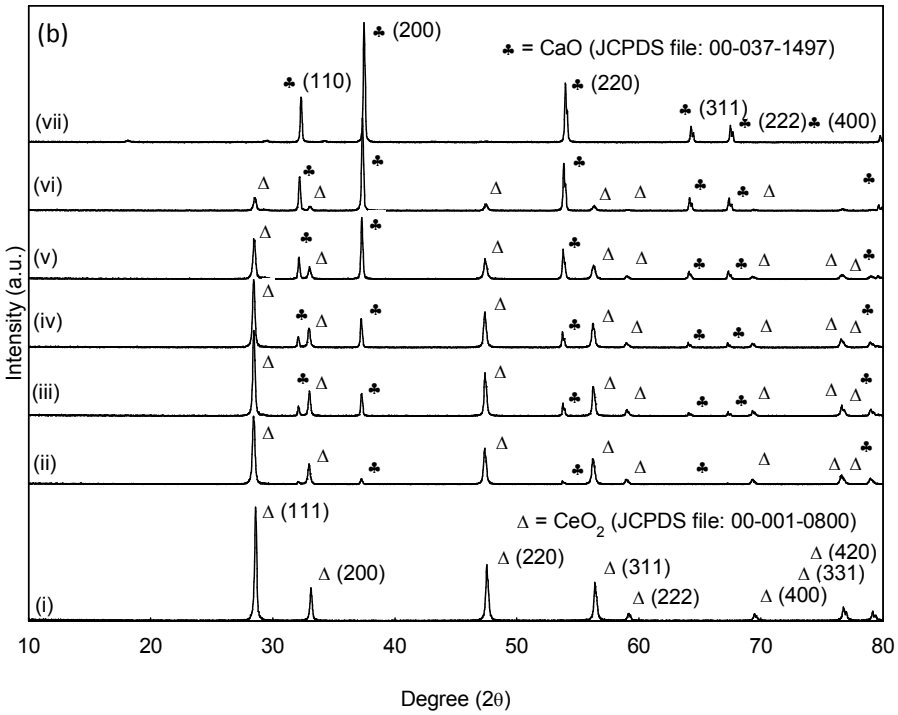

Fig. 3 X-ray diffraction patterns of (a) CeO_2 (i), CaCe4.00-pH9 (ii), CaCe4.00-pH10 (iii), CaCe4.00-pH11 (iv), CaCe4.00-pH12 (v) and CaO (vi) catalysts; (b) CeO_2 (i), CaCe0.25 (ii), CaCe0.67 (iii), CaCe1.00 (iv), CaCe4.00 (v), CaCe19.0 (vi) and CaO (vii) catalysts. ♣, characteristic peak of CaO and Δ, characteristic peak of CeO_2.

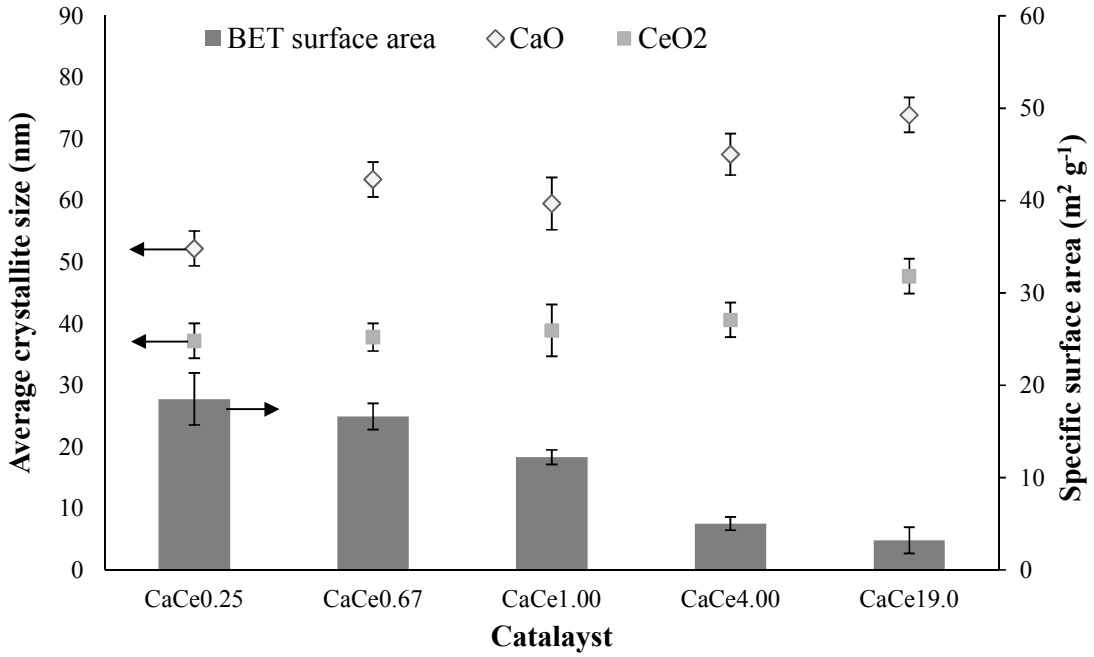

Fig. 4 Crystallites sizes and BET surface area of CaO-CeO_2 mixed metal oxides.

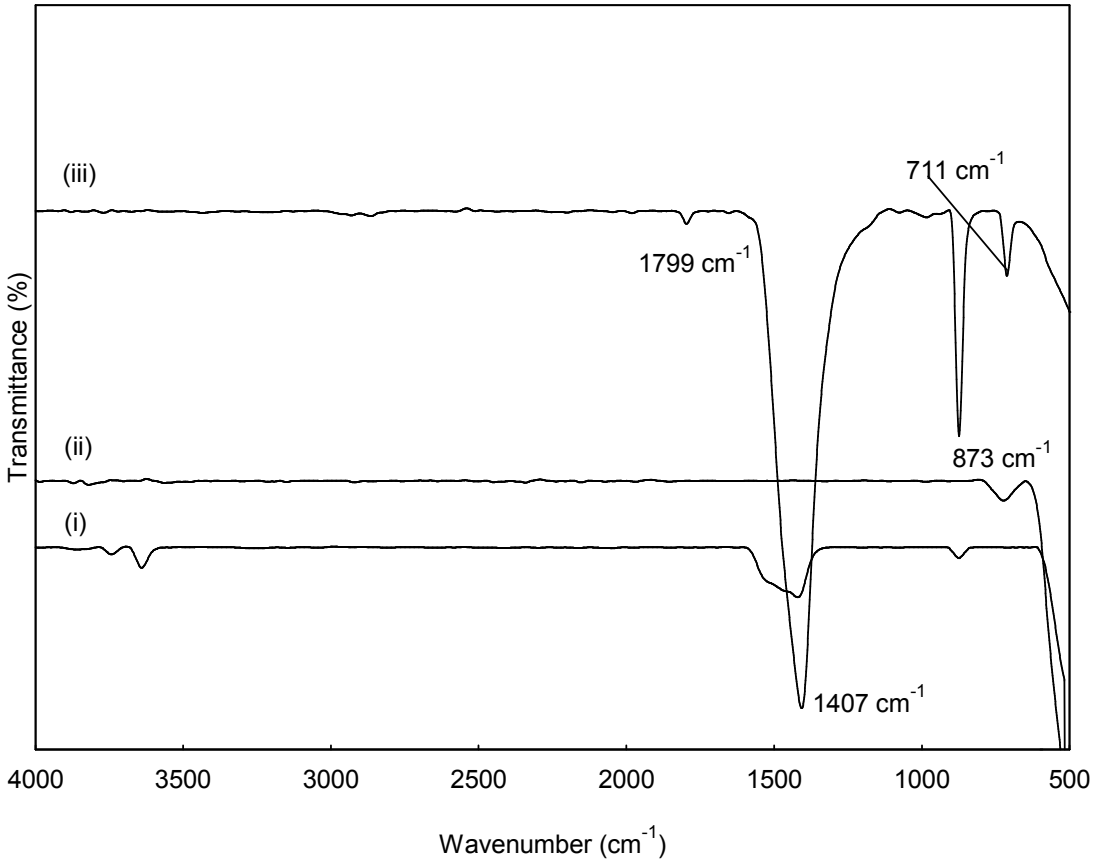

Fig. 5 FTIR spectrum of CaO (i) CeO_2 (ii) and CaO-CeO_2 (iii) catalysts.

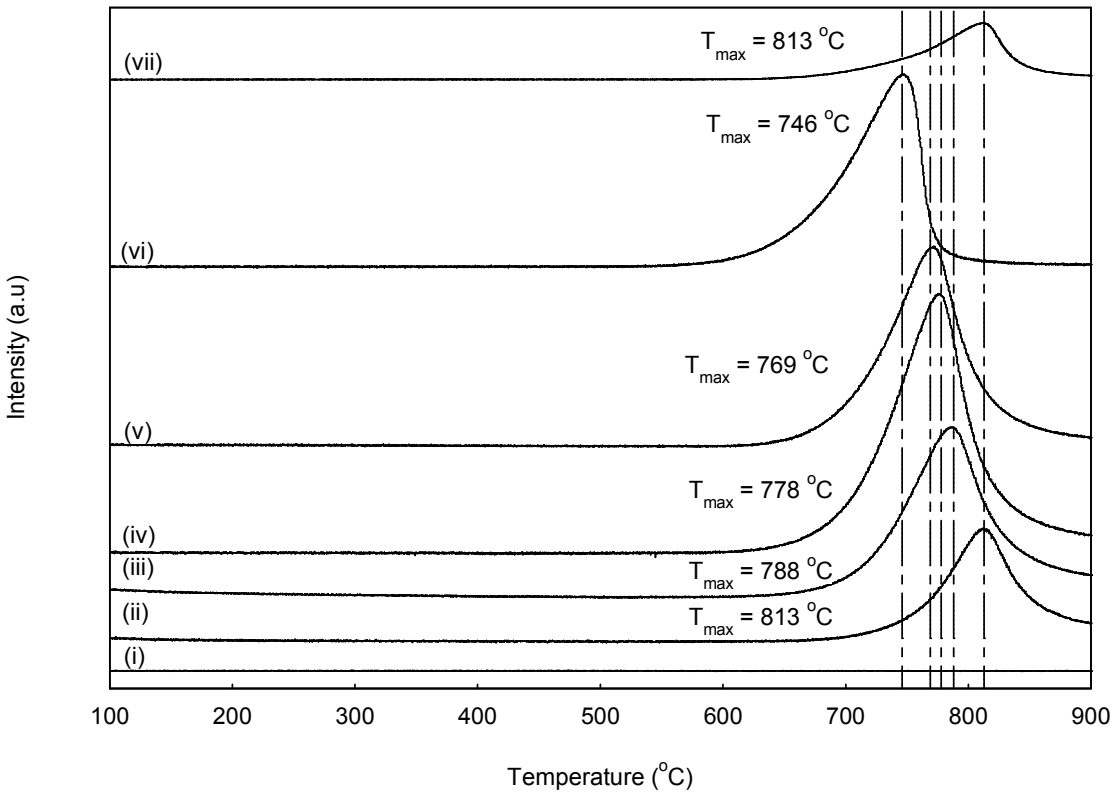

Fig. 6 CO_2-Temperature programmed desorption profiles of CeO_2 (i), CaCe0.25 (ii), CaCe0.67 (iii), CaCe1.00 (iv), CaCe4.00 (v), CaCe19.0 (vi) and CaO (vii) catalysts.

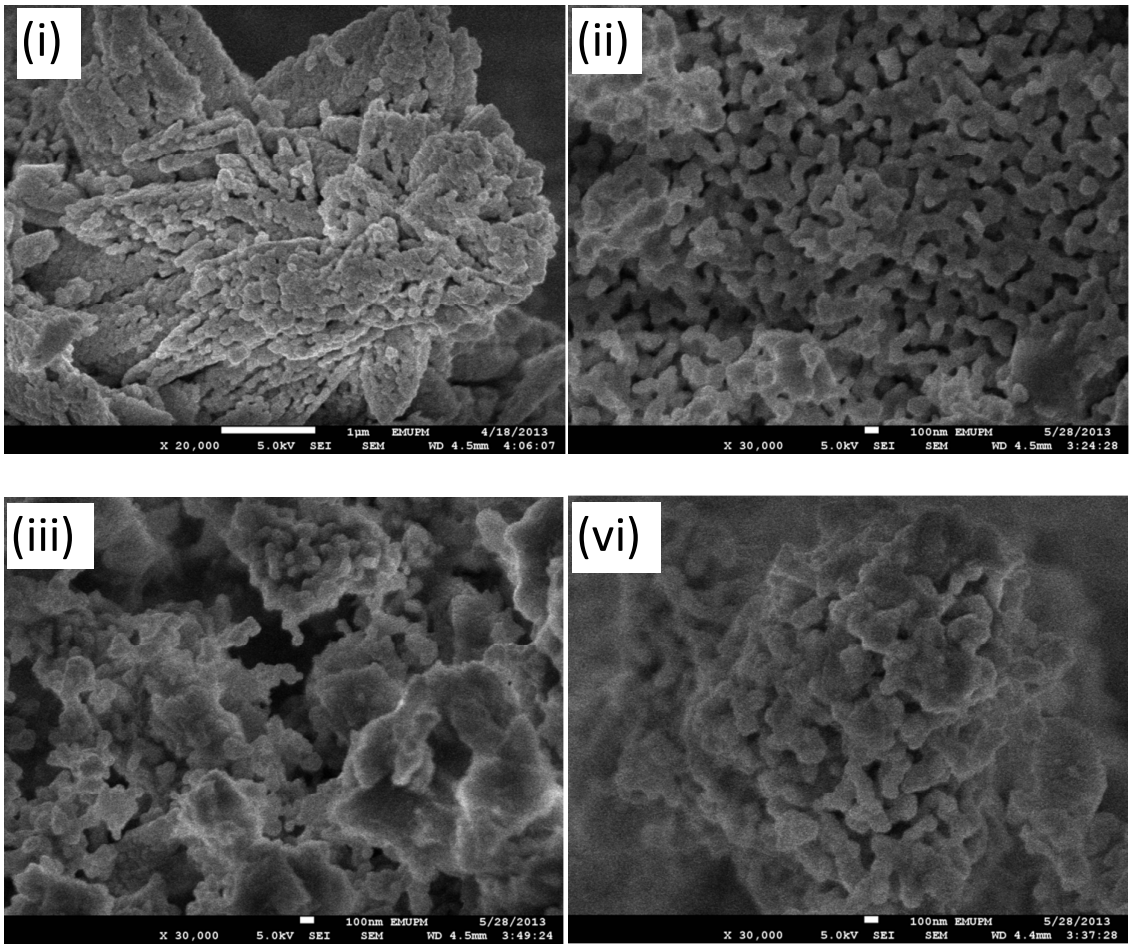

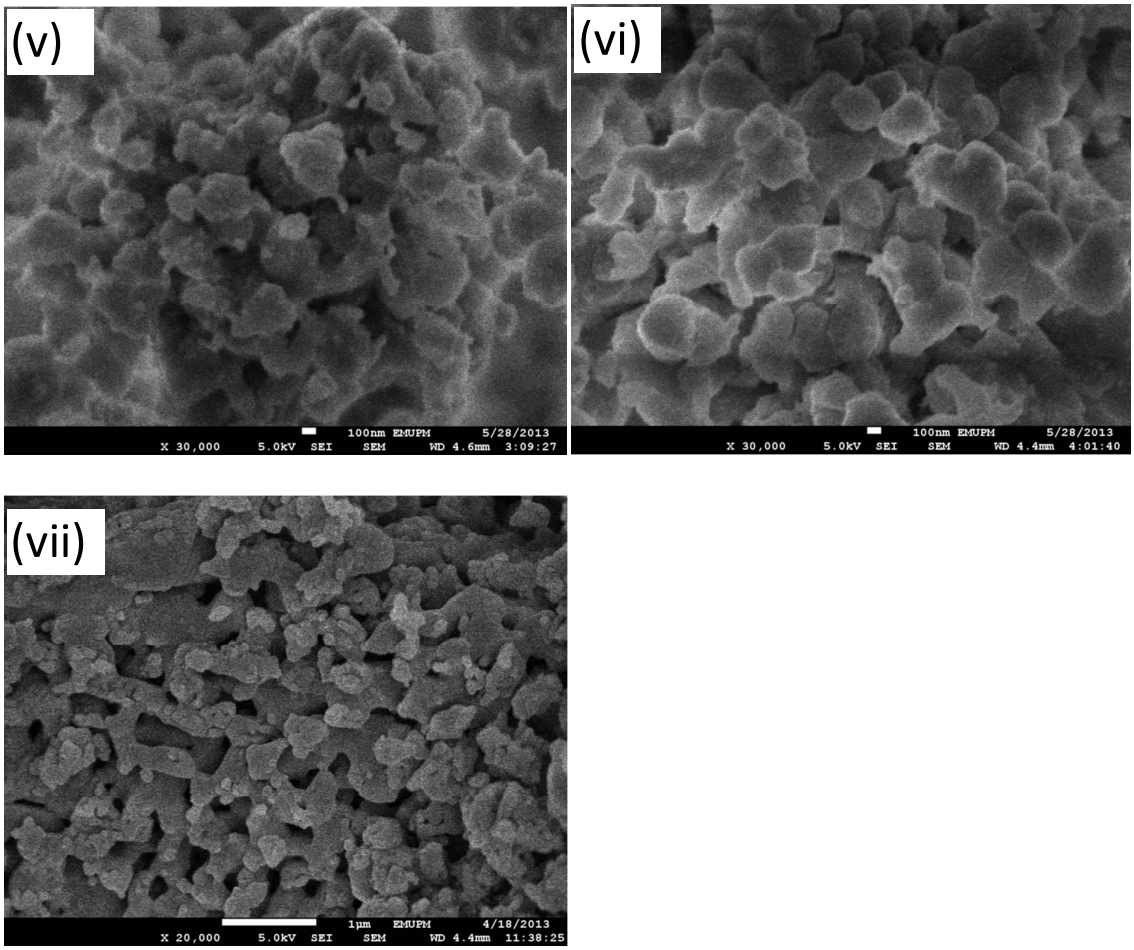

Fig. 7 SEM micrographs of CaO (i), CaCe0.25 (ii), CaCe0.67 (iii), CaCe1.00 (iv), CaCe4.00 (v), CaCe19.0 (vi), and CeO_2 (vii) catalysts.

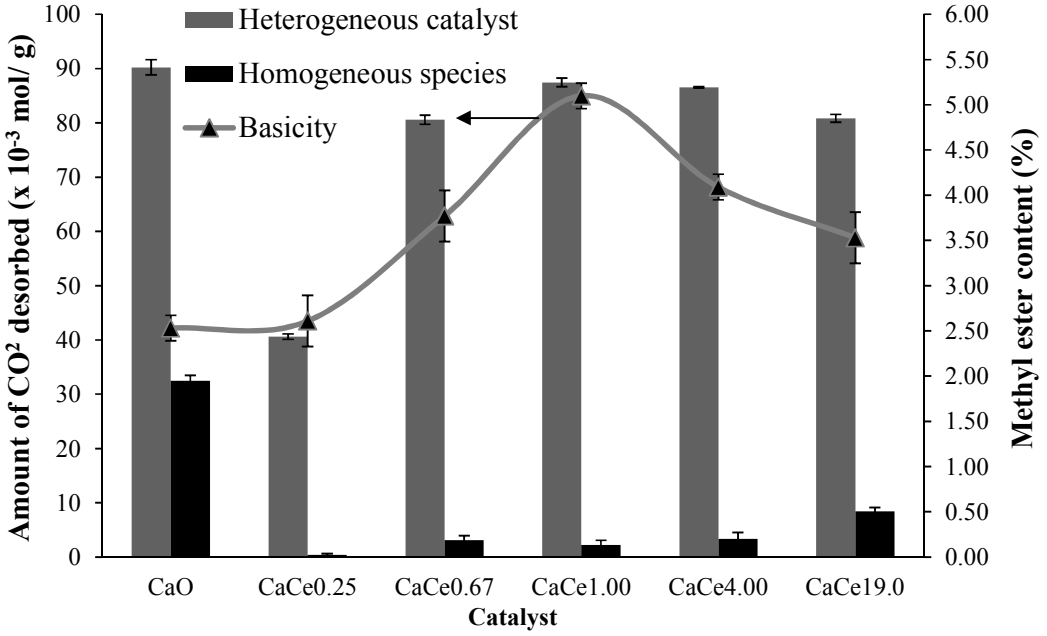

Fig. 8 Catalytic performance of CaO-CeO_2 catalysts with different Ca/Ce molar ratios: (a) using heterogeneous catalyst, (b) using homogeneous species presence in methanol solution and (c) basicity of CaO-CeO_2 catalysts. Transesterification condition: oil= 10 g, *n*(methanol):*n*(oil) = 12:1, catalyst dosage = 4 wt. %, reaction time = 6 h, reaction temperature = 65 °C.

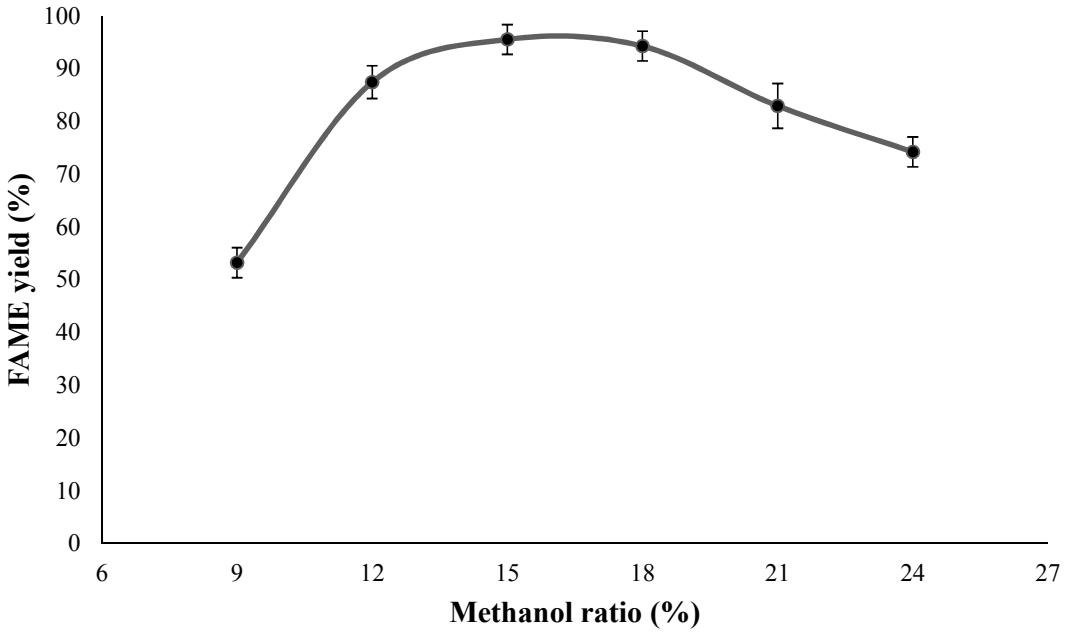

Fig. 9 Effect of methanol/oil ratio on the FAME yield of crude JCO. Reaction condition: oil= 10 g, catalyst dosage = 4 wt. %, reaction time = 6 h, reaction temperature = 65 °C.

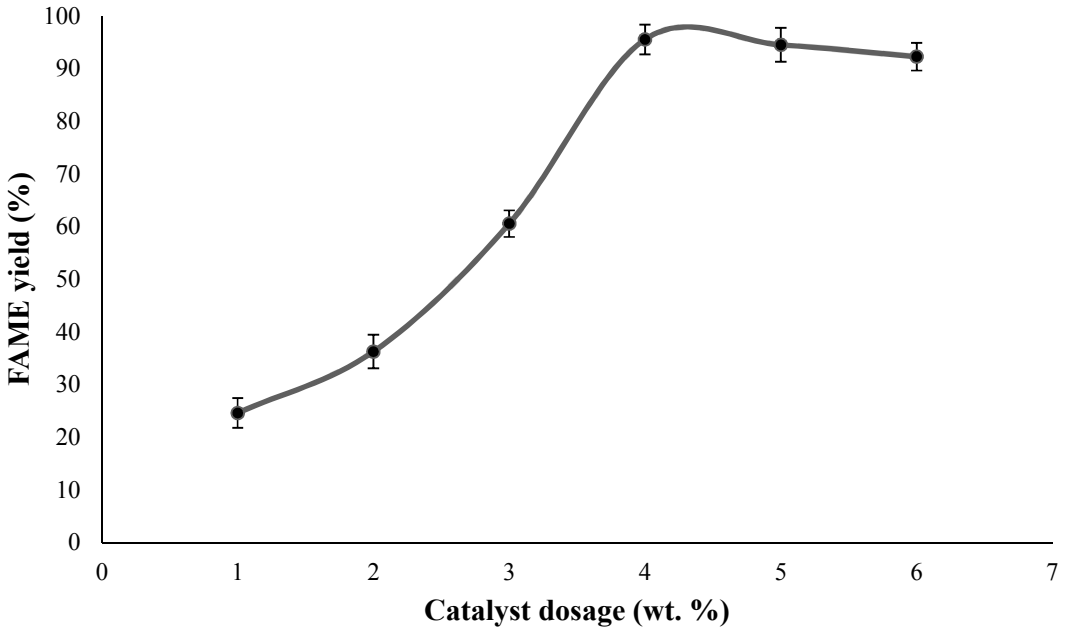

Fig. 10 Effect of catalyst loading on the FAME yield of crude JCO. Reaction condition: oil= 10 g, (methanol):(oil) = 15:1, reaction time = 6 h, reaction temperature = 65 °C.

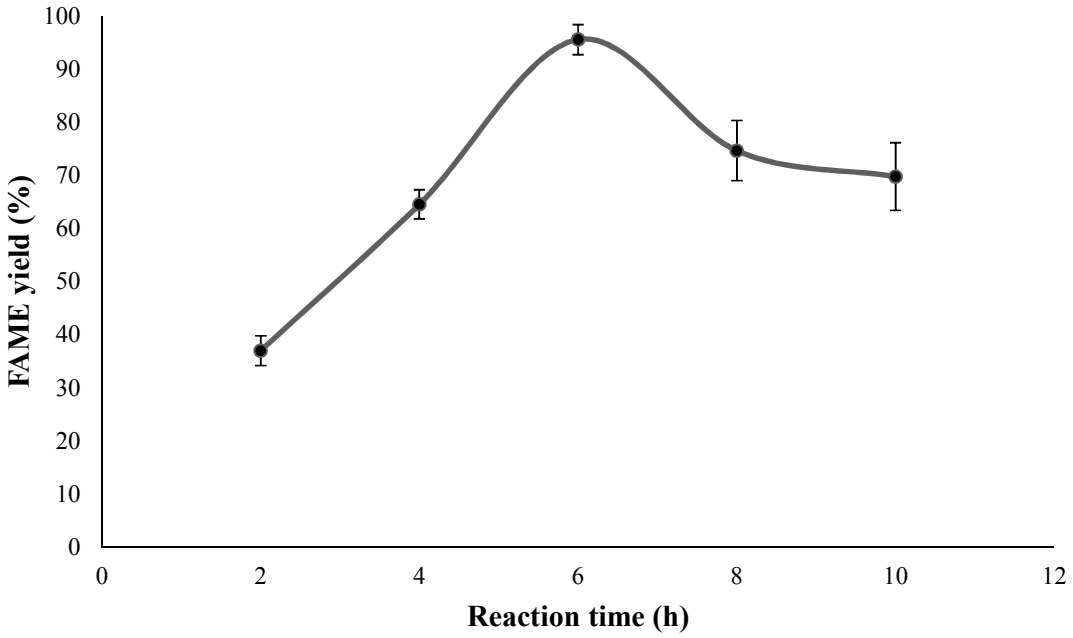

Fig. 11 Effect of reaction time on the FAME yield of crude JCO. Reaction condition: oil= 10 g, (methanol):(oil) = 15:1, catalyst dosage = 4 wt. %, reaction temperature = 65 °C.

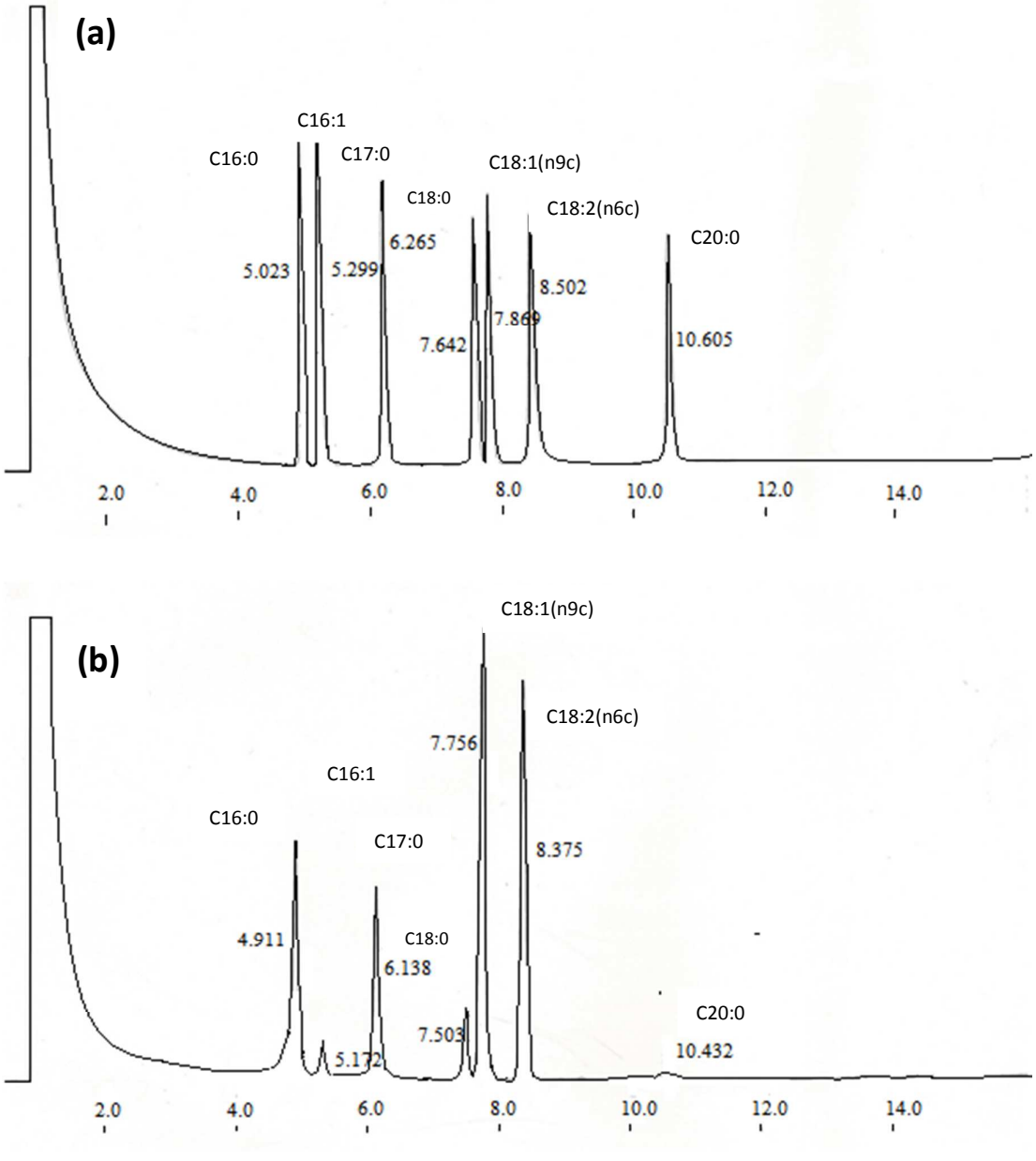

Fig. 12 Gas chromatography of (a) standard references of fatty acid methyl esters (1000 ppm) and (b) transesterification of jatropha derived biodiesel (FAME).

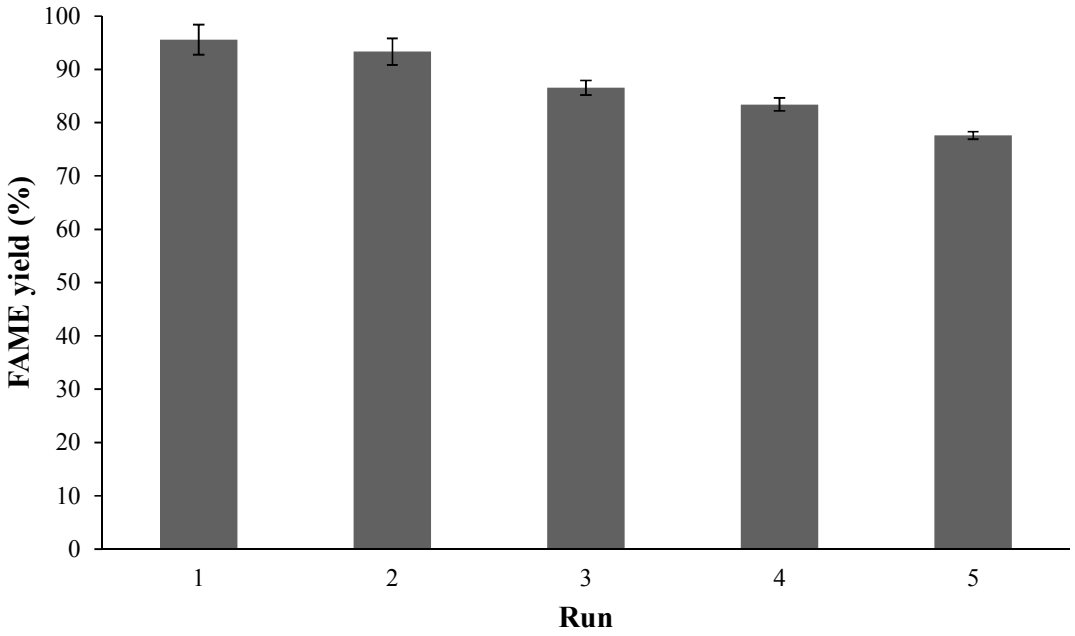

Fig. 13 Recyclability study of catalyst [Reaction condition: Oil = 10 g, catalyst dosage = 4 wt. %, (methanol):(oil) = 15:1, reaction time = 6 h].